



Gold-Silver Catalysts: Ruling Factors for Establishing Synergism

Marta Stucchi,^[a] Andrea Jouve,^[a] Alberto Villa,^[a] Gergely Nagy,^[b] Miklòs Németh,^[b] Claudio Evangelisti,^[c] Rodolfo Zanella,^[d] and Laura Prati*^[a]

DPU and SOL immobilisation have been used to prepare 1% AuAg/TiO₂ with internal ratio 1:1 and 4:1 which have been studied as fresh, calcined in air at 300 °C and reduced at 550 °C in H₂. TEM-EDS, XPS, UV-Vis and CO-DRIFT allowed to characterize the samples in terms of particle size, particle composition, exposure and oxidation state of metals. Correlating these characteristics to the catalytic behaviour we concluded that only Au-rich catalysts show synergistic effect, silver in bimetallic

systems appears more resistant to oxidation than in monometallic one, thermal treatment enhances the SMSI thus producing (regardless to the post-treatment) almost the same amount of Au^{δ+} and also Ag^{δ+}. Catalysts prepared by DPU (calcined in air or reduced in H₂) are more active than SOL (fresh or calcined) probably due to the higher presence of gold at the surface.

1. Introduction

Gold catalysts proved to be a sustainable choice for the selective oxidation of alcohols.^[1] Catalytic oxidation reactions allow converting bio-renewable feedstock to higher-valued chemicals and they are at the base of the current production of petrochemicals from not-exhaustible sources.^[2] Glycerol is a highly functionalized bio-renewable molecule, coming as by-product from the production of biodiesel.^[3] The selective transformation of glycerol allows obtaining many valued products, so much that glycerol is expected to become one of the major renewable building block chemicals thus consisting a platform molecule. Glycerol can be oxidized to glyceric acid, tartronic acid, glycolic acid, oxalic acid and other important chemical intermediates (Figure 1), hence its conversion opens significant new markets in polymers, ethers and other fine compounds.^[4]

Many papers already reported that gold particle size is crucially important in determining the activity and the selectivity in glycerol oxidation, being particles in the range 2–


5 nm more active than 10–30 nm, which in turn are more selective toward glyceric acid.^[5,6] However, monometallic Au suffers from deactivation due to nanoparticle sintering or to the formation of carbonyl compounds irreversibly adsorbed on the active sites of the catalysts.^[7–10] Many papers reported the synergistic effect of bimetallic structures in different catalytic reactions, such as PtCu alloys,^[11,12] or PtPd alloys^[13] compared to monometallic Pt. As well as Y. Wang et al.^[14] reported a synergistic effect in a bimetallic structure of ZnO and TiO₂. The use of gold-based bimetallic catalysts have shown to overcome a lot of these problems, enhancing activity, stability, and selectivity.^[15] In particular, Ag was studied as a second metal for improving the catalyst activity and resistance.^[16] Recent studies by Mou^[16] and Zanella^[17] proved that in CO oxidation AuAg particles are more active than monometallic ones, thus showing synergistic effect. The addition of one metal to another can produce a large diversity in the structure and morphology of NPs. The nanoparticle composition has a strong influence on the catalytic activity, but also its structure such as disordered/ordered, segregated, or core-shell, plays a role modulating the material features and its behaviour.^[17] Although it is clear that the extent of alloying in bimetallic systems influences catalytic activity and selectivity, understanding the origin of this effect is still lacking.^[18] Theoretical studies^[19] investigated the segregation of Ag in Au–Ag NPs, reporting that segregation is composition, size and temperature dependent. In agreement with this, Slater et al.^[20] studied Ag–Au nanoparticles with controlled compositions and structures through the combination of STEM imaging with EDX spectroscopy, showing that nanoparticle surface segregation inverts from Au-rich to Ag-rich as Au content increases.^[20] On the other hand, segregation in bimetallic particles can be also influenced by the synthetic route and by post-treatments. Zanella et al.^[17] studied Au–Ag bimetallic catalysts supported on TiO₂ by sequential deposition–precipitation method, with 4 wt.% gold loading and various amounts of silver proving the synergistic effect between gold and silver. It was also shown that catalyst activation


[a] Dr. M. Stucchi, A. Jouve, Dr. A. Villa, Prof. L. Prati
Università degli Studi di Milano
Dipartimento di Chimica
via C. Golgi 19, 20133 Milano, (Italy)
E-mail: Laura.Prati@unimi.it

[b] G. Nagy, M. Németh
Centre for Energy Research
Surface Chemistry and Catalysis Department
PO Box 49, H-1525 Budapest, (Hungary)

[c] Dr. C. Evangelisti
CNR, Istituto di Scienze e Tecnologie Molecolari (ISTM)
via G. Fantoli 16/15, 20138 Milano (Italy)

[d] Prof. R. Zanella
Instituto de Ciencias Aplicadas y Tecnología
Universidad Nacional Autónoma de México
Circuito Exterior S/N, C. U., 04510, Mexico City (Mexico)

 Supporting information for this article is available on the WWW under <https://doi.org/10.1002/cctc.201900591>

 This manuscript is part of the Special Issue dedicated to the Women of Catalysis.

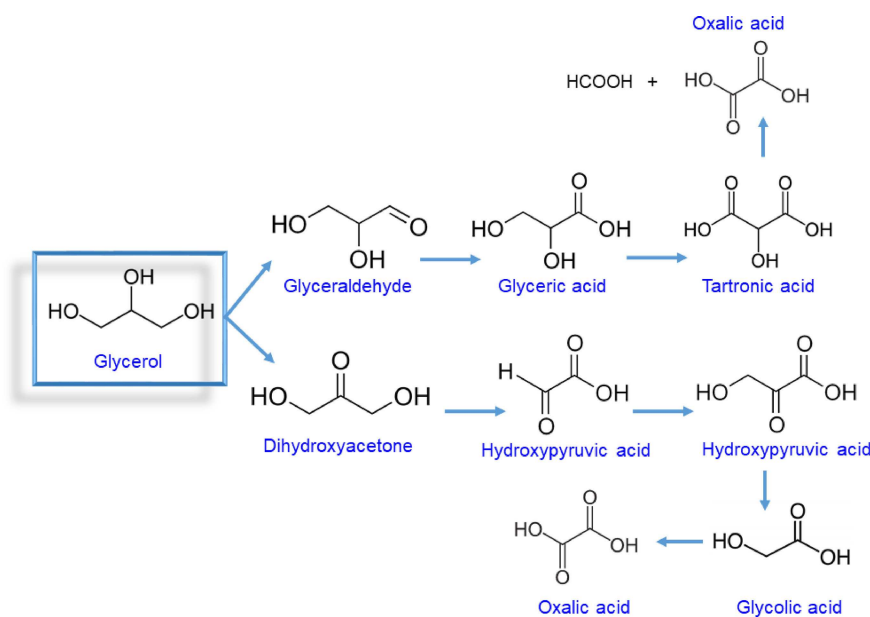


Figure 1. Pathways for glycerol selective oxidation.

temperature influenced the catalytic activity in correlation with different nanoparticles composition.^[21]

Recently we reported the different behaviour in glycerol oxidation of Au–Ag catalysts supported on alumina, synthesized by SOL immobilization and SMAD (Solvent Metal Atom Dispersion) method.^[22] Even both preparations showed synergistic effect between the two metals, a different metal distribution was revealed depending on preparation method and post treatments, which rebounded on different catalytic activity.

Based on these facts and considering the already proven efficiency of Au–Ag bimetallic catalysts in glycerol oxidation, here we compared the catalytic activity and selectivity of differently synthesized and post-treated Au/Ag–TiO₂ catalysts. Synthesis by deposition precipitation with urea (DPU) was compared with sol-immobilization synthesis. The effect of calcination and reduction treatments has been investigated as a function of the catalyst preparation method and Au/Ag atomic ratio (1:1 and 4:1).

Experimental Section

General

HAuCl₄·3H₂O, AgNO₃ (purity > 99.0%), polyvinyl alcohol (PVA) (MW = 9000–10,000, 80% hydrolysed), poly(diallyldimethylammonium)chloride (PDDA, medium molecular weight) aqueous solution, 20 wt.% and NaBH₄ (purity ≥ 98%) were from Sigma-Aldrich. TiO₂ (P25 by Degussa) was the support. Glycerol (86–89 wt.% solution), glyceric acid and all the intermediates were from Sigma-Aldrich. Deionized water (Milli-Q purified) was used in all the experiments. Gaseous oxygen from SIAD was 99.99% pure.

Synthesis by Sol Immobilization

In sol-immobilization (SOL) synthesis, bimetallic AuAg sol were prepared by reduction of the precursors by NaBH₄ in aqueous solution in presence of polyvinyl alcohol (PVA) as stabilizing agent and the support was added after nanoparticles formation.^[23,24] Bimetallic AuAg sols were prepared by consecutive reduction of the AgNO₃ and HAuCl₄, with Au/Ag molar ratio equal to 1:1 and 4:1, respectively. Firstly, we mixed AgNO₃ and PVA solution (0.2 wt.%) in MilliQ water, adding after a freshly prepared 25 mM NaBH₄ solution. The appearance of a yellow colour confirmed the reduction of Ag. The solution was stirred for 30 minutes, then HAuCl₄ mixed with PVA solution (0.2 wt.%) added and just at once further 25 mM NaBH₄ under vigorous stirring. Solution changed colour to brown.

The appropriate amount of sol and TiO₂ providing 1.0 wt% metal loading of final AuAg/TiO₂ was mixed and the adsorption of nanoparticles was favoured by addition of proper amount of PDDA solution (0.08 wt.%). The suspension was stirred at room temperature for 2 h, in order to have the complete adsorption of the metal nanoparticles on the support surface, which was indicated by the complete decolouration of the liquid phase. The powder was then filtered, washed with water, and dried at 80 °C overnight.

Synthesis by Deposition-Precipitation

Ag was first deposited by deposition-precipitation with NaOH (DPNaOH) followed by the deposition of Au by DPU. For that TiO₂ was added to an aqueous solution of AgNO₃ heated at 80 °C. The pH was adjusted to 9 by dropwise addition of NaOH (0.5 M), in order to promote the precipitation of AgOH on the support. The suspension was kept under stirring for 2 h at 80 °C. Gold was deposited by DPU^[24,25] method after drying the Ag/TiO₂ under vacuum at 80 °C for 2 h. The final metal loading (Ag + Au) is 1 wt.% for all the samples.

Post-Treatments

Calcination was carried out at 300 °C for 1 h in a tubular furnace and static air. Heating rate was 5 °C min⁻¹, and at the end of the treatment sample cooled down to RT. Reduction occurred at 300 °C or 550 °C for 1 h in a tubular furnace, under H₂ flow. Temperature was reached through a heating rate of 5 °C min⁻¹ under N₂ flow, as well as free cooling until RT occurred under N₂ flow. The DPU reduced samples were first activated in a flow of hydrogen with a heating rate of 2 °C/min up to 550 °C followed by a plateau at the same temperature of 2 h.

The complete samples list is reported below (Table 1).

Sample name	Synthesis Method	Au/Ag	Post-Treatment
Au ₁ Ag ₁ /TiO ₂ _SOL	Sol immobilization	1:1	As prepared
Au ₁ Ag ₁ /TiO ₂ _SOL_calc	Sol immobilization	1:1	300 °C in air
Au ₁ Ag ₁ /TiO ₂ _DPU	DPU	1:1	As prepared
Au ₁ Ag ₁ /TiO ₂ _DPU_red	DPU	1:1	550 °C in H ₂
Au ₄ Ag ₁ /TiO ₂ _SOL	Sol immobilization	4:1	As prepared
Au ₄ Ag ₁ /TiO ₂ _SOL_calc	Sol immobilization	4:1	300 °C in air
Au ₄ Ag ₁ /TiO ₂ _DPU	DPU	4:1	As prepared
Au ₄ Ag ₁ /TiO ₂ _DPU_calc	DPU	4:1	300 °C in air
Au ₄ Ag ₁ /TiO ₂ _DPU_red	DPU	4:1	550 °C in H ₂

Characterization Analysis

UV-Vis Spectroscopy

UV-visible spectra of fresh and the variously pretreated supported catalysts were recorded by an Agilent Cary 60 spectrometer with a DRA accessory in diffuse reflectance to measure the localized surface plasmon resonance (LSPR) of metallic nanoparticles.

X-ray Photoelectron Spectroscopy (XPS)

The catalyst samples pretreated variously ex situ were measured by XPS using a KRATOS XSAM 800 XPS machine for the determination of surface composition and oxidation state of the metals. Al K α characteristic X-ray line, 40 eV pass energy and FAT mode were applied for recording the XPS lines of Au 4f, Ag 3d, O 1s, C 1s, Ti 2p regions and Ag MNN Auger peaks. Ti 2p_{3/2} binding energy at 458.6 eV was used as reference for charge compensation. The Auger parameter (AP) of silver was calculated as the sum of the kinetic energy of Ag M₅N₄₅N₄₅ Auger lines and the binding energy of Ag 3d_{5/2} peak.

Diffuse Reflectance Infrared Fourier Transform Spectroscopy (DRIFTS)

The top surface of the samples was probed by CO adsorption at room temperature followed by DRIFTS. Spectra were collected by a Nicolet iS50 infrared spectrometer equipped with an MCT detector, a Specac DRIFT accessory and a Specac environmental chamber with a ZnSe window. 64 scans were collected with a resolution of 4 cm⁻¹. CO adsorption was measured in the flow of 1%CO/Ar after 5 minutes on as prepared or variously pre-treated samples, and the state just before CO addition was used as background. The spectra were presented as log(1/R), where R was the reflectance, and the

CO gas spectrum was subtracted. The as prepared samples were measured after 10 min under Ar flow in the DRIFT cell, the ex situ prepared ones after a short (5 min) refreshing in situ pre-treatment at the same temperature, and there were also longer subsequent pre-treatments applied in situ. The in situ pre-treatments were performed under synthetic air or 5% H₂/Ar flow with 10 °C/min heating rate and after a given isothermal period with cooling down to room temperature in air and Ar flow, respectively.

TEM and EDS Analyses

Electron micrographs were carried out using a ZEISS LIBRA200FE microscope equipped with a 200 kV FEG source. Energy-dispersive X-ray spectra (EDS-Oxford INCA Energy TEM 200) and elemental maps were collected along with HAADF-STEM (high angular annular dark field scanning transmission electron microscopy) micrographs. Before the analysis, the samples were finely smashed in an agate mortar, suspended in isopropanol and sonicated, then each suspension was dropped onto a holey carbon-coated copper grid (300 mesh) and the solvent was evaporated. Histograms of the particle size distribution were obtained by counting onto the TEM micrographs at least 300 particles; the mean particle diameter (d_m) was calculated by using the formula $d_m = \sum d_i n_i / \sum n_i$ where n_i was the number of particles of diameter d_i .

Catalytic Oxidation of Glycerol

Glycerol oxidation reaction occurred at 50 °C and 3 bar of O₂, in a 30 mL glass reactor, equipped with heater, mechanical stirrer, gas supply system and thermometer. 10 mL of glycerol 0.3 M and NaOH (NaOH/Glycerol ratio = 4, mol/mol) solution was transferred in the reactor, to which the catalyst was added in order to have a glycerol/metal ratio of 2000, mol/mol. Reaction started when the temperature of 50 °C was reached. Oxygen pressure was kept controlled by a mass flowmeter. Sampling occurred periodically, analysing samples by high-performance liquid chromatography (HPLC) using a column Alltech OA-10308 (300 mm × 7.8 mm) with UV and refractive index (RI) detection. The eluent was a H₃PO₄ 0.1% wt. solution.

2. Results

2.1 Characterization of 1%Au₁Ag₁/TiO₂

1% Au₁Ag₁/TiO₂ was synthesized by sol-immobilisation and sequential DPU method.^[17,21] The evolution of the bimetallic particles as a function of the different post-synthesis treatments (i.e. calcination, reduction with H₂) has been investigated.

As evidenced by HAADF-STEM/EDS analysis, the SOL preparation provided bimetallic particles already in the as prepared (fresh) catalyst (Figure 2). The average composition of the particles resulted very close to the nominal value (Au atomic % = 48.5 ± 5). However, as visible on Figure 3, the LSPR band of the as prepared bimetallic Au₁Ag₁/TiO₂_SOL does not show the blue shift compared to that of the corresponding monometallic Au/TiO₂ towards that of Ag/TiO₂ (451 nm) due to AuAg alloying as expected.^[13,17] Both appears at about 533 nm, on the contrary, that the LSPR of parent Au₁Ag₁ sols at 489 nm was about 30 nm lower than the LSPR of the Au sol. In supported form likely due to drying and storing in air the

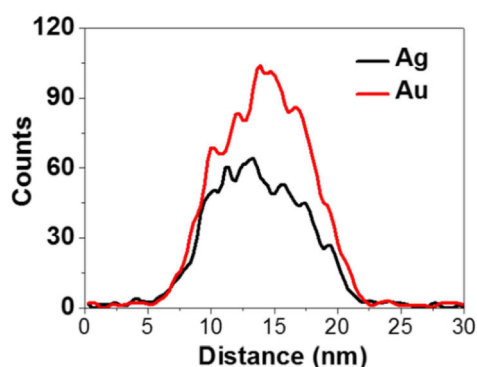
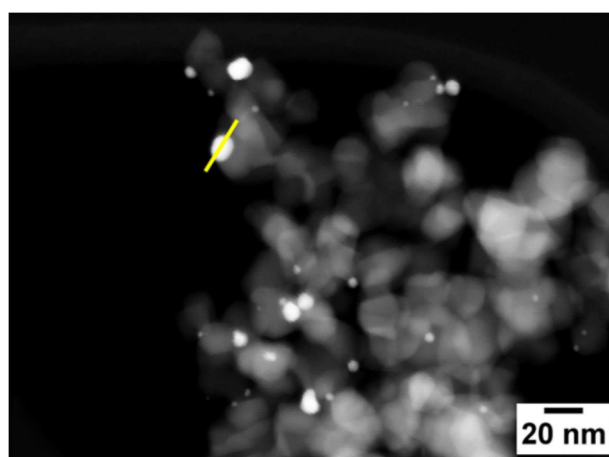


Figure 2. Representative HAADF-STEM micrograph (top) and EDS particle profile of the selected particle (bottom) of SOL-derived Au₁Ag₁/TiO₂ (as prepared).

surface Ag was oxidized somewhat causing a red shift (as was observed on O₂ contact at room temperature of freshly reduced Ag/TiO₂^[21]) compensating the blue shift resulting from alloying. The UV-vis spectra of the as prepared Au₁Ag₁/TiO₂_DPU and the corresponding monometallic samples show only very weak LSPR bands suggesting the presence of Au and Ag dominantly in oxidised form. In DPU samples gold and silver reduced extensively above 80 °C, and the formation of bimetallic nanoparticles was reported to start over 155 °C.^[17] At temperatures higher than 155 °C, the plasmon shifts to lower wavelength (515 nm at 300–350 °C) between that of silver (475 nm) and that of gold (530 nm), confirming the formation of bimetallic particles.^[17]

In calcined state the enhanced intensity LSPR band of Au₁Ag₁/TiO₂_SOL and Au/TiO₂_SOL was red shifted compared to the as prepared state, in lower extent in the case of Au/TiO₂. The larger intensity indicates particle size increase,^[26] that is in agreement with the particle size determined by TEM (Figure 4). The original 2.7 nm mean diameter changed to 5.3 nm during calcination (see in Table 2). The red shift might be due to the removal of organic residues from the Au(Ag) NPs accompanied with an enhanced interaction with the support, plus in case of the bimetallic sample likely due to an extended oxidation of surface silver. The SOL derived Ag/TiO₂ decolourized in calcination, its LSPR disappeared, silver must be oxidized. In the

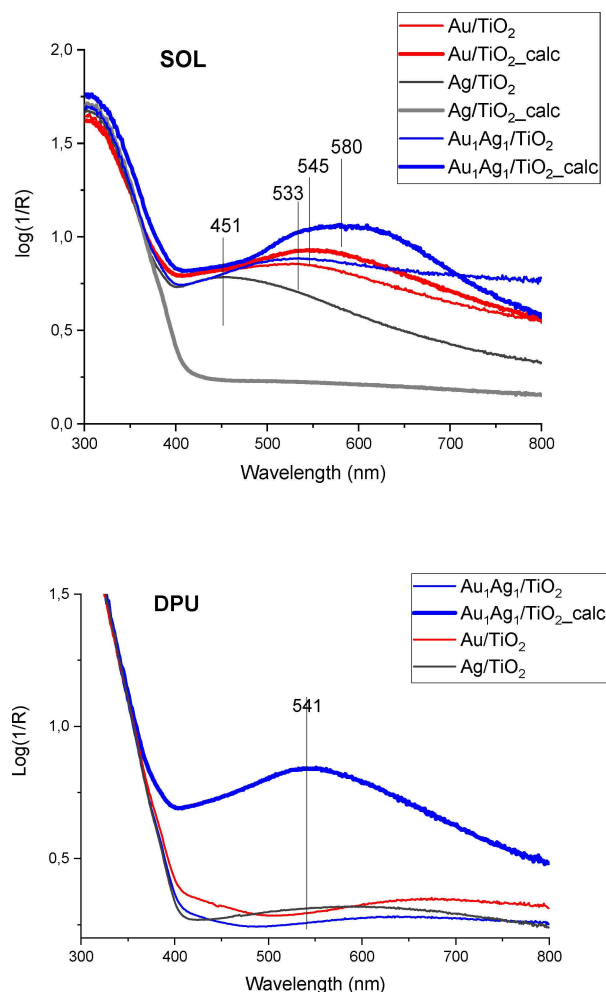


Figure 3. UV-vis of Au₁Ag₁/TiO₂_SOL (top image) and Au₁Ag₁/TiO₂_DPU (bottom image) before and after calcination. Monometallic Au and Ag are reported as reference.

calcination of DPU derived Au₁Ag₁/TiO₂ plasmonic NPs evolved indicated by LSPR band (541 nm) at somewhat lower wavelength than measured for calcined Au/TiO₂_SOL (545 nm) as a result of reduction of Au and Ag and also alloy formation.

Studying by XPS (Table 2) the surface composition, monometallic SOL samples showed that even after calcination Au is not fully reduced and a fraction of Au^{δ+} is still present (Au⁺/Au⁰=0.21). This could be partially ascribed to the interaction with TiO₂. The fresh bimetallic SOL showed a Ag enrichment at the surface (Au/Ag atomic ratio 0.63). In this case Au is rather in Au^{δ+} state and Ag presented an Auger parameter (719.5) consistent with the metallic state as well according to Ferrara et al.,^[27] that reported AP=720.5, 717.8 and 718.4 for metallic silver, Ag₂O and AgO. After calcination, we observed particle growth (from 2.7 nm to 5.3 nm) (Figures 4) and Ag appeared not totally oxidized as the AP (718.4) assumes an intermediate value between the one of metallic and the oxidized one. However, in calcined SOL Ag/TiO₂ (AP=717.7) silver is oxidized. Also, Au, as in the monometallic sample, is partially present as Au^{δ+} in almost the same ratio (0.26) as in

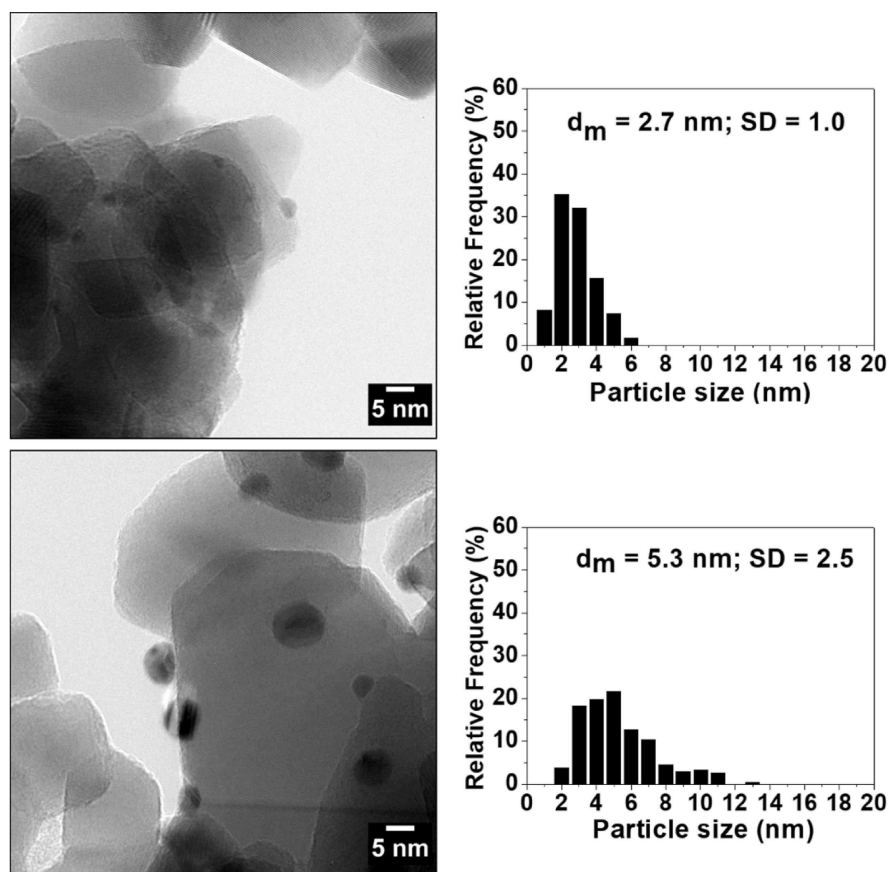


Figure 4. Representative HRTEM micrograph and histogram of particle size distribution of SOL-derived Au₇Ag₇@TiO₂ fresh (top) and calcined (bottom).

Table 2. XPS analysis of Au₇Ag₇/TiO₂ by sol-immobilization and DPU. Comparison between the fresh and calcined catalysts.

Catalyst	Mean diam. [nm]	Binding Energy [eV]		Atomic ratio		Ag MNN K.E.	Auger parameter
		Ag 3d _{5/2}	Au 4f _{7/2}	Au/Ag	Au ^{δ+} /Au ⁰		
Au/TiO ₂ _SOL_calc	–	–	Au ^{δ+} 84.5	Au ⁰ 82.6	Au ^{δ+} /Au ⁰ 0.21	–	–
Ag/TiO ₂ _SOL_calc	–	368.8	–	–	–	348.9	717.7
Au ₇ Ag ₇ /TiO ₂ _SOL	2.7 ± 1.0	368.7	84.8	–	–	0.63	350.8
Au ₇ Ag ₇ /TiO ₂ _SOL_calc	5.3 ± 2.5	367.9	84.8	82.7	0.26	0.34	350.5
Au ₇ Ag ₇ /TiO ₂ _DPU ^[a]	–	368.0	87.1	85.0	–	–	–
Au ₇ Ag ₇ /TiO ₂ _DPU_red ^[a]	2.6 ± 1.0	368.2	–	84.0	–	2.5	–

[a] values reported by Zanella et al.^[21]

the previous case. This finding indicates a reciprocal interaction between Ag and Au possibly mediated by TiO₂ able to install strong metal-support interaction (SMSI). Moreover, the thermal treatment, as expected, increased the enrichment of Ag at the surface (Au/Ag at.% 0.34).

DPU-derived catalysts, already reported by Zanella et al.,^[21] in the fresh state showed two peaks for Au (4f_{7/2}) at 87.1 and 85.0 eV (Table 2). The peak at B.E. 87.1 eV refers to Au^{III}, due to the formation of a Au^{III}-urea complex on TiO₂; the one at 85.0 was attributed to Au^I, addressed to the reduction of part of the Au^{III} species under XPS beam. The binding energy value of Ag (3d_{5/2}) at 368.0 eV is between those of Ag⁰ and Ag⁺, ascribed by the Authors to partial reduction due to the XPS experiments.

After in situ reduction, Au is in the metallic form, and we expected that also Ag is completely reduced. The DPU samples presented Au/Ag ratios particularly high with respect to the nominal ones (3.3 in the fresh and 2.5 in the reduced) highlighting Au enrichment at the surface which decreased due to the thermal (reducing) treatment. The particularly high value compared to the nominal one was also addressed to Ag partial segregation as AgCl^[17] on titania surface and Au as Au^{III}-urea complex^[24] with no interaction between each other. To note that DPU sample after the thermal treatment is characterized by smaller particle size than the SOL ones (2.6 nm vs 5.3 nm).

Distribution and oxidation state of the metals were also studied by CO-DRIFT experiments (Figure 5a–b). To note that

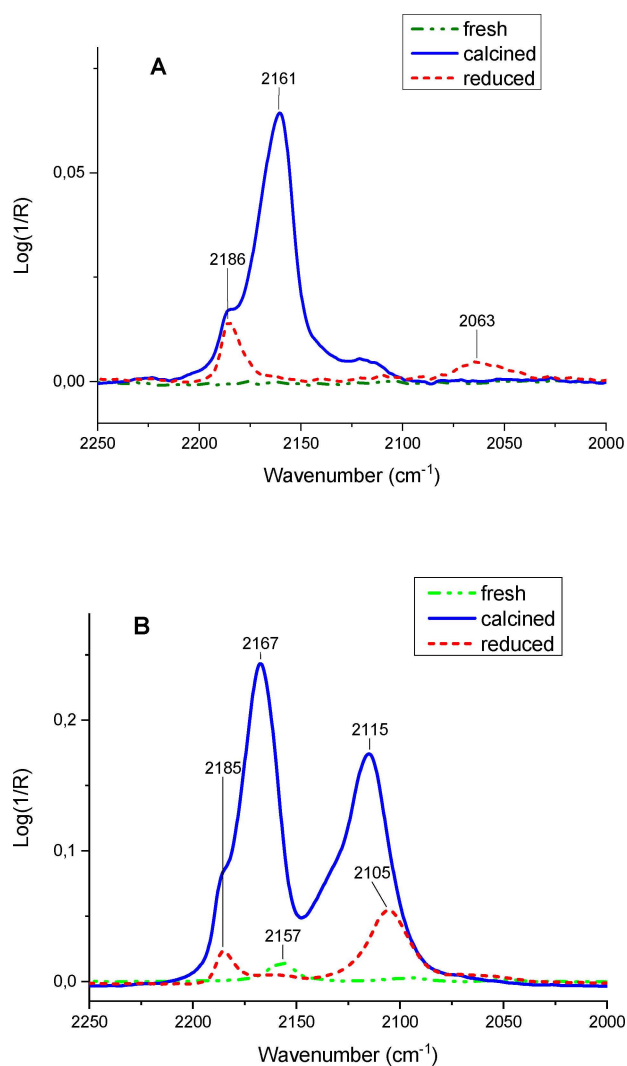


Figure 5. DRIFT measurement of CO adsorption at room temperature on Au_4Ag_1 supported on TiO_2 by SOL (top image) and DPU (bottom image). Comparison between fresh (green line), reduced (red line) and calcined (blue line) samples.

CO is very weakly adsorbed on Ag^0 species. The band at 2105 cm^{-1} refers to $\text{Au}^0\text{-CO}$ species.^[28] The frequency of 2055 cm^{-1} corresponds to CO adsorbed on Ag^0 , while the band at 2160 cm^{-1} refers to Ag^+ . Comparing SOL and DPU-prepared samples, CO signals in SOL catalysts appeared generally weaker than in the DPU ones. This behaviour can be connected to the presence of PVA molecules adsorbed on the SOL-samples surface thus limiting the adsorption of CO.

The CO adsorption bands helped in the interpretation of XPS results. In the SOL (Figure 5a) we did not observe any signals in the fresh sample due to the presence of PVA and eventually PDDA residues and water thus limiting the CO adsorption (green line). This result is also consistent with XPS that indicates a surface where Ag^0 is covering the Au^0 . After calcination Ag is oxidized even partially (XPS) and a strong peak at 2161 cm^{-1} due to CO adsorbed on Ag^+ appeared (blue line). Au^0 is almost submerged by Ag in agreement with XPS Au/Ag

ratio that decreases after calcination with respect to the original fresh sample value. DPU (Figure 5b) reduced sample (red line) presented only the peak at 2105 cm^{-1} due to the presence of metallic Au whereas after calcination (blue line) both peaks (2115 and 2167 cm^{-1}) related to Au^0 and Ag^+ . A shoulder at 2132 cm^{-1} ascribed to $\text{Au}^{\delta+}$ appears. The results are in agreement with XPS data if we consider the double contribution of Gold (0 and $\delta+$) compared to the Ag signal. Here the amount of gold at the surface is higher than the silver.

2.2 Characterization of 1% Au_4Ag_1

As well as the Au/Ag 1:1 samples, $\text{Au}_4\text{Ag}_1/\text{TiO}_2$ were fully characterized as prepared, after calcination and after reduction with H_2 .

UV-VIS analysis of SOL samples (Figure 6) showed also in the case of 4:1 as in case of 1:1 composition discussed earlier

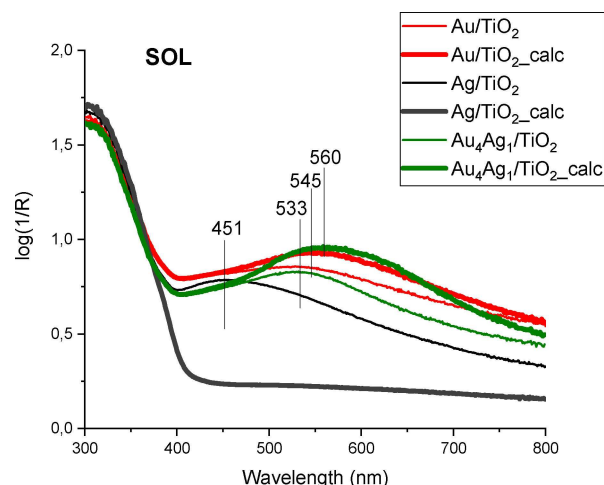


Figure 6. UV-vis of $\text{Au}_4\text{Ag}_1/\text{TiO}_2\text{-SOL}$ before and after calcination.

the plasmon peak at about the same wavelength (533 nm) in as prepared state and red shifted (560 nm) compared to monometallic Au/TiO_2 (545 nm) in calcined state, instead of blue shift due to alloying. Similar explanation applies here as earlier. The Ag segregated and partially oxidized on the surface of the bimetallic particles, but in lower extent than on 1:1 case results in larger red shift than the alloying in opposite direction.

For DPU samples UV-Vis spectra (Figure 7) did not show any peak for fresh samples (no metallic nanoparticles) as expected, whereas a plasmon band appeared after reduction or calcination also at 560 nm like in case of the corresponding SOL sample.

1% $\text{Au}_4\text{Ag}_1/\text{TiO}_2$ fresh sample prepared by SOL showed mean particle size larger than the fresh sample prepared by DPU (mean diameter = 2.9 nm and 1.1 nm, respectively) (Figures 8 and 10). Moreover, particle size resulted differently affected by calcination treatment. After calcination, SOL sample showed a broader particle size distribution with a mean

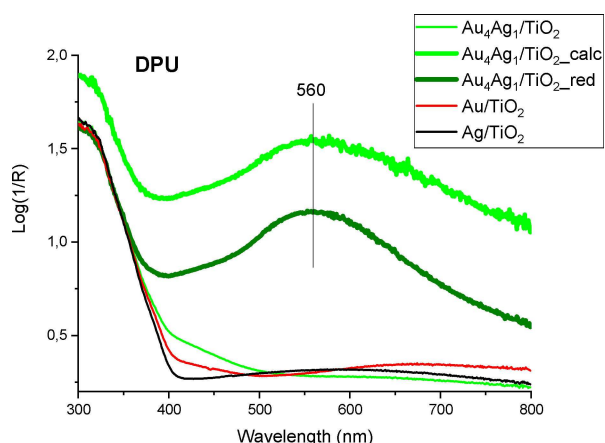


Figure 7. UV-vis of DPU-derived catalysts after different treatments.

diameter of 5.1 nm (Figure 8 bottom), whereas in the case of DPU sample, the particle size increased till 2.4 nm, with a particle size distribution considerably narrower than the sol case (Figure 10 bottom). AuAg particles in SOL-derived catalysts showed an average Au/Ag molar ratio of 4.6 calculated on EDS analysis on single particle, which is similar to the nominal one. In the case of DPU-derived catalysts, EDS analysis revealed an average Au/Ag molar ratio of 7.3 (Figure 11), higher than the

nominal one, which can be explained, as in the case of 1:1 Au:Ag sample, with a partial segregation of Ag as AgCl. Indeed, in the survey XPS spectrum the binding energy of Cl p_{3/2} for metal chloride appears at ~198.5–199 eV that could be associated to the presence of chlorides of AgCl. Bimetallic particles were gold-rich at the surface.

XPS analyses (Table 3) showed in the fresh Au₄Ag₁/TiO₂ prepared by DPU the presence of gold in the Au^{III} and Au^I form (B.E 87.3 eV and 84.8 eV) as in the case of the 1:1.^[24] The Au³⁺/Au⁺ ratio evidenced the higher contribution of Au⁺ than of Au³⁺. The AP of Ag (721) is particularly high indicating the presence of at least partially reduced oxidation state. The ratio between Au and Ag (9.1) indicates a very high exposure of Au. Reduction in H₂ at high temperature (550 °C) decreases the Au/Ag ratio to 4.2 (similar to the nominal value), confirming the migration of Ag atoms toward the surface of nanoparticle. Au is not fully reduced and Au^{δ+}/Au⁰ is 0.23. Ag presents an AP decreased with respect to the one of the fresh counterpart that could indicate a partial oxidation of Ag as for Au. Interestingly, calcination in air forms the same distribution of species except for the Ag/Au ratio that resulted higher than the one obtained by reduction (6.4 vs 4.2). The two catalysts thus differ from the Au exposure at the surface but apparently in both cases Ag and Au are present with the same oxidation states. Our opinion is that TiO₂ is able to interact with the metals through the thermal treatment provoking strong support-metal interaction thus

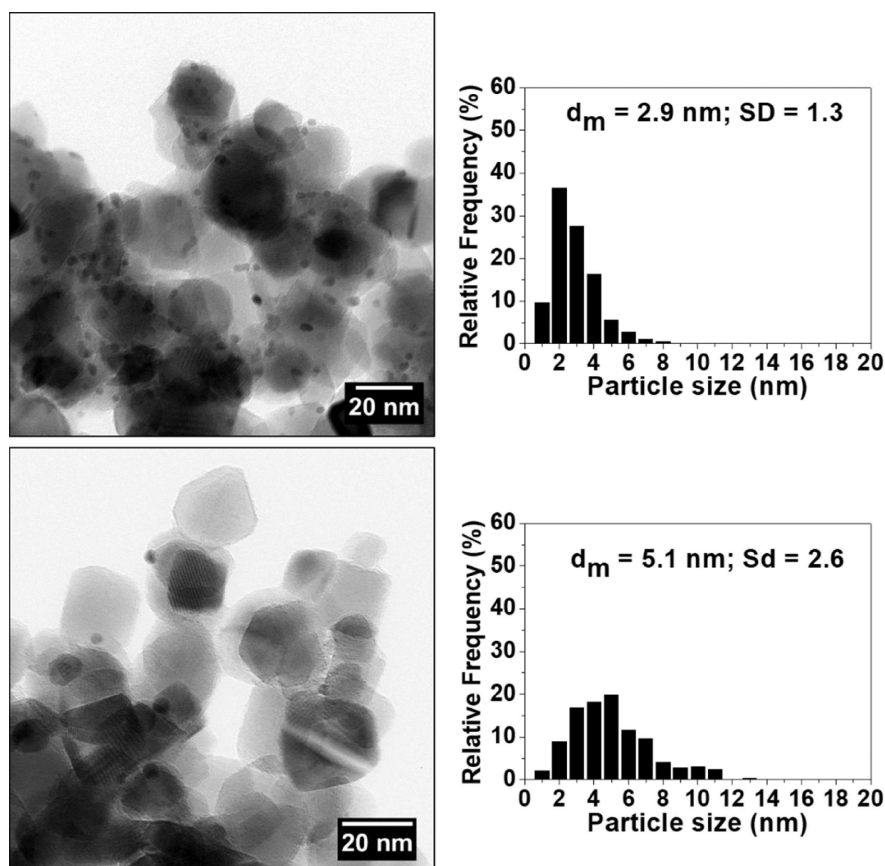


Figure 8. Representative HRTEM micrograph and histogram of particle size distribution of SOL-derived Au₄Ag₁/TiO₂ fresh (top) and calcined (bottom).

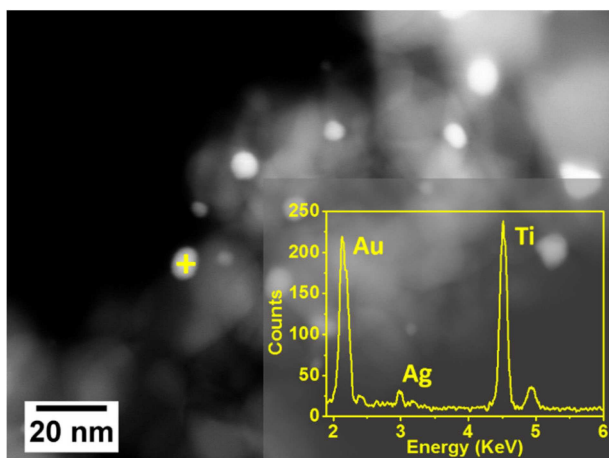


Figure 9. HAADF-STEM micrograph and EDS spectrum (inset) carried out on a single particle SOL-derived $\text{Au}_4\text{Ag}_1/\text{TiO}_2$ calcined.

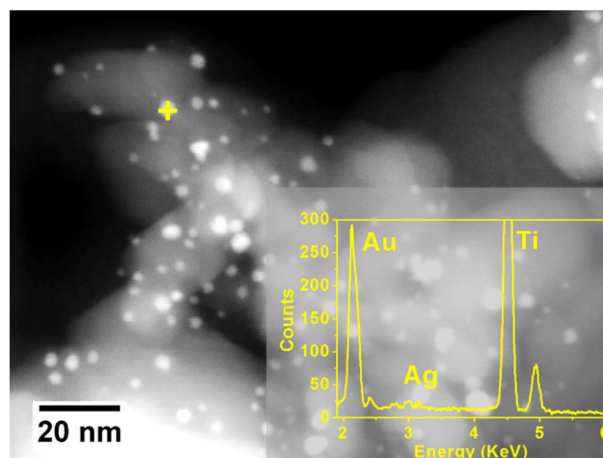


Figure 11. HAADF-STEM micrograph and EDS spectrum (inset) carried out on a single particle DPU-derived $\text{Au}_4\text{Ag}_1/\text{TiO}_2$ calcined.

providing the same distribution of oxidation numbers regardless the atmosphere. In the case of $\text{Au}_4\text{Ag}_1/\text{TiO}_2$ prepared by SOL immobilization, again a $\text{Au}^{\delta+}/\text{Au}^0$ ratio around 0.27 is obtained thus confirming the important role of the support in determining the presence of $\text{Au}^{\delta+}$. The Au/Ag atomic ratio was 3.6 similar to the nominal value in the fresh sample, but it

increased to 4.7 after calcination. These values are very similar to the one obtained by EDS-TEM analysis, confirming the alloyed nature of the bimetallic particles (Figure 9). As in the case of DPU, the APs of silver indicate in both cases (fresh and calcined) a similar oxidation state which is not sensitive to the treatment.

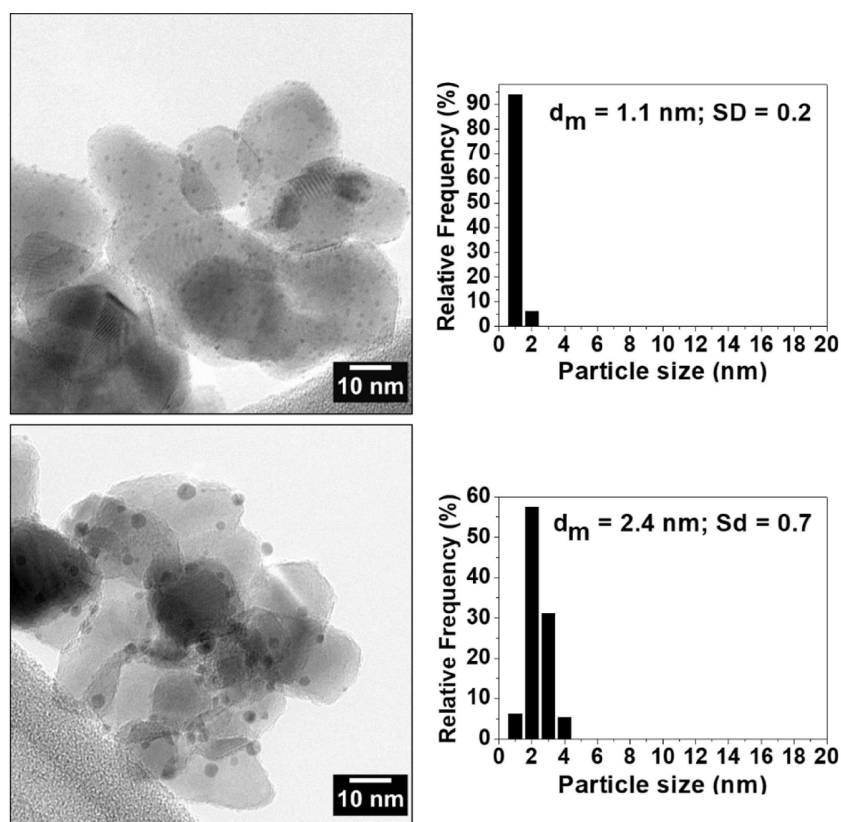
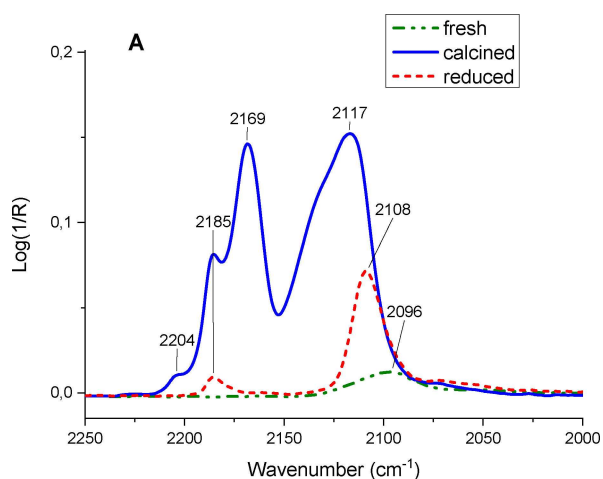
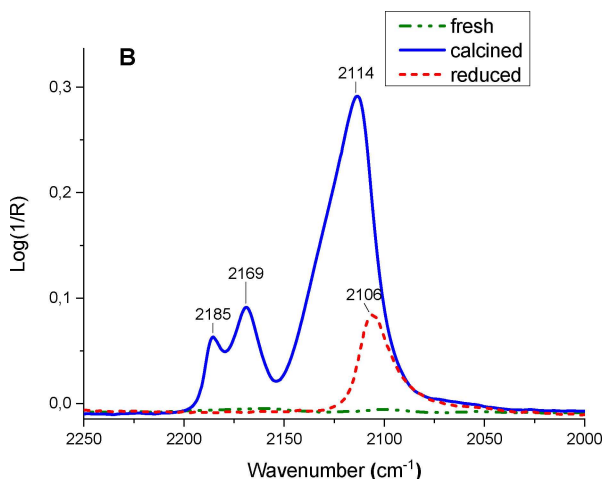


Figure 10. Representative HRTEM micrograph and histogram of particle size distribution of DPU-derived $\text{Au}_4\text{Ag}_1/\text{TiO}_2$ fresh (top) and calcined (bottom). (Calcination at 300°C in air or in H_2 gave the same result).

Table 3. XPS analysis of Au₄Ag₁/TiO₂ by sol-immobilization and DPU. Comparison between the catalysts as prepared and the catalysts after calcination and reduction treatments.

Catalyst	Mean diam. [nm]	Binding Energy [eV]			Ti 2p _{3/2}	Atomic ratio Au/Ag	Ag MNN K.E.	Auger Parameter
		Ag 3d _{5/2}	Au 4f _{7/2}	Au 4f _{7/2}				
Au ₄ Ag ₁ /TiO ₂ _DPU	1.1 ± 0.2	368.1	Au ³⁺ 87.2 Au ^{δ+}	Au ⁺ 84.8 Au ⁰	Au ^{3+/Au+} 0.46 Au ^{δ+/Au⁰}	458.6	9.1	352.9 721.0
Au ₄ Ag ₁ /TiO ₂ _DPU_red	2.4 ± 0.7	366.9	85.4	83.0	0.23	458.6	4.2	352.9 719.8
Au ₄ Ag ₁ /TiO ₂ _DPU_calc	2.4 ± 0.7	367.0	85.4	83.2	0.29	458.6	6.4	352.4 719.4
Au ₄ Ag ₁ /TiO ₂ _SOL	2.9 ± 1.3	367.7	86.2	83.8	0.26	458.6	3.6	353.0 720.7
Au ₄ Ag ₁ /TiO ₂ _SOL_calc	5.1 ± 2.6	367.3	86.0	83.4	0.28	458.6	4.7	352.8 720.1

**Figure 12.** DRIFT measurement of CO adsorption at room temperature on Au₄Ag₁ supported on TiO₂ by SOL. Comparison between fresh (green line), reduced (red line) and calcined (blue line) samples.**Figure 13.** DRIFT measurement of CO adsorption at room temperature on Au₄Ag₁ supported on TiO₂ by DPU. Comparison between fresh (green line), reduced (red line) and calcined (blue line) samples.

To confirm these findings, we studied the behaviour of CO adsorption by DRIFT analyses (Figures 12 and 13).

CO-DRIFT measurements on SOL catalysts (Figure 12) revealed only a weak peak at 2096 cm⁻¹ which can indicate Au in the metallic state but shielded by the protective agent (PVA).

The peak due to adsorption of CO on Au⁰ becomes more important after calcination (2117 cm⁻¹) with a shoulder at 2132 cm⁻¹ that can be addressed to the presence of partially oxidized Au. Ag⁺ is also detected in the calcined sample with the peak at 2169 cm⁻¹. Considering the double contribution of CO adsorbed on Au in different oxidation state, the result is consistent with the Au/Ag measured by XPS (0.26).

In the case of DPU samples, the CO-DRIFT spectra (Figure 13) indicated a situation similar to the SOL catalysts. The fresh DPU catalyst (green line) showed no peaks. After reduction (red line) the peak correlated to the presence of Au⁰ appeared at 2106 cm⁻¹. No signals for Ag were detected. Considering that by XPS we obtained the same AP by reduction or calcination of DPU sample (meaning Ag in the same oxidation state), but after calcination a clear signal due to the presence of Ag⁺ appeared, we concluded that in the reduced sample Ag⁺ signal is lost due to the lower intensity of signals. Calcination shifted the peak of Au⁰ at 2114 cm⁻¹ with the presence, as in the case of SOL, of a shoulder at 2132 cm⁻¹. The peak of Ag⁺ appeared at 2169 cm⁻¹. In agreement with the XPS analyses, the relative ratio between Au and Ag in the DPU samples appeared higher than in the SOL samples.

2.3 Catalytic Activity in Glycerol Oxidation

All the catalysts prepared by DPU and by SOL were tested in the selective glycerol oxidation under mild conditions (50 °C, 3 bar of O₂, glycerol/metal ratio of 2000 mol/mol, NaOH/glycerol of 4). 1%Au₁Ag₁/TiO₂ catalysts (not reported in Table 4) didn't show any activity even if Au monometallic catalysts resulted active. In the case of monometallic Au, the catalytic behaviour of SOL calcined is similar to the one of DPU reduced (1662 vs 1679 h⁻¹).

However, when Au/Ag ratio was 4:1, catalysts not only became active in glycerol oxidation (Table 4) but they also showed synergistic effect by the combination of the two metals. Considering that 1:1 samples are inactive regardless metal distribution (gold rich surface in DPU and silver rich surface in SOL) and metal oxidation state (fresh, calcined, reduced), we concluded that the synergistic effect (and therefore the activity) derived from a delicate balance between the two metals on the surface of the nanoparticles, where the relative ratio represents a fundamental ruling factor.

Catalyst	Initial activity ^[a] [h ⁻¹]	GLY conv. [%] (at 3 h)	Glyceric	Tartronic	Glycolic	Formic	Oxalic
1%Au/TiO ₂ _SOL_fresh	245	33	48.6	12.5	7.3	3.4	–
1%Au/TiO ₂ _SOL_calc	1662	90	64.0	–	4.0	6.3	–
1%Au/TiO ₂ _DPU_fresh	–	–	–	–	–	–	–
1%Au/TiO ₂ _DPU_red	1679	85	56.0	–	–	10.0	–
1%Au ₄ Ag ₁ /TiO ₂ _DPU	–	–	–	–	–	–	–
1%Au ₄ Ag ₁ /TiO ₂ _DPU_calc	2113	81.9	56.8	12.2	9.6	6.1	2.4
1%Au ₄ Ag ₁ /TiO ₂ _DPU_red	1524	86.4	51.3	17.7	5.2	2.9	4.0
1%Au ₄ Ag ₁ /TiO ₂ _SOL	892	59.8	68.7	6.5	9.8	7.7	3.0
1%Au ₄ Ag ₁ /TiO ₂ _SOL_calc	1616	62.7	52.1	16.5	14.9	10.4	2.7

[a] Initial activity has been calculated after 15 min calculated as mol converted per mol of metal (h⁻¹). [b] Selectivity at 3 h reaction.

Considering the initial activity (conversion at 15 min) we observed that the most active catalyst was 1% Au₄Ag₁/TiO₂ DPU_calc (2113 h⁻¹) followed by the SOL_calc (1616 h⁻¹). In this latter case it should be noted that the almost double activity of SOL catalyst obtained by calcination of the fresh sample, cannot be ascribed only to the removal of the protective agent^[29] considering also the growing of the particle size due to the thermal treatment (Table 3). The enlargement of the particle size should reduce the activity thus playing an opposite role compared to the removal of PVA. Looking at reaction profiles (Figure 14) we could also note the similarities of the catalytic

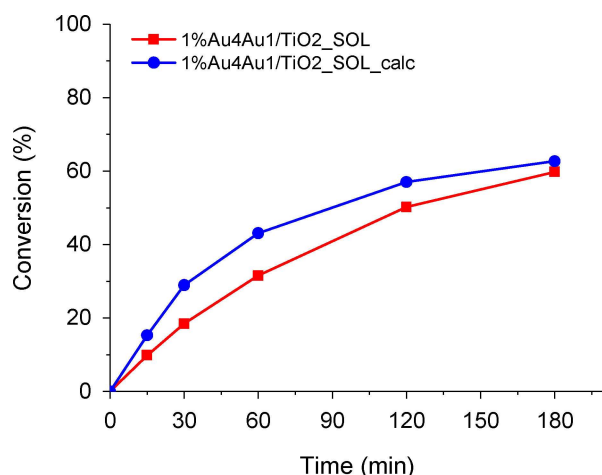


Figure 14. Glycerol conversion over time by 1% Au–Ag (4:1) supported on TiO₂ by SOL. Comparison between 1%Au₄Ag₁/TiO₂_SOL as a) not treated (red squares), b) calcined (blue dots).

behaviour between fresh and calcined SOL sample being the conversion after 3 h quite similar regardless the presence of PVA and the particle size (2.4 vs 5.1 nm). XPS revealed that calcination varied the surface composition which appeared slightly richer in Au (Table 3).

Also considering 1% Au₄Ag₁/TiO₂ prepared by DPU, the catalysts in both treated state (reduced and calcined) despite different initial activity behaved similarly (Figure 15) both showing a conversion of glycerol around 80% in 3 h. The characterisation of the two catalysts by TEM and XPS appeared

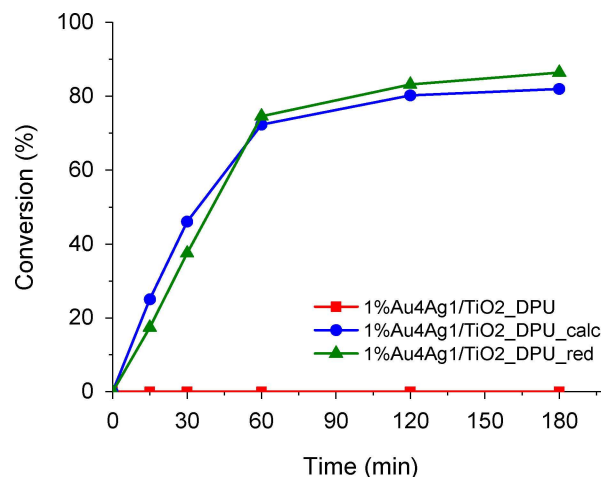


Figure 15. Glycerol conversion over time by 1% Au–Ag (4:1) supported on TiO₂ by DPU. Comparison between a) not treated (red squares), b) calcined (blue dots) and c) reduced (green triangles).

very similar. The not treated as prepared state is inactive. As the thermal profile is the same, we thought that in this case the SMSI should be the same.

Comparing DPU and SOL synthesis, 1% Au₄Ag₁/TiO₂ by DPU were generally more active and reached higher glycerol conversion after 3 h. From the selectivity point of view all the catalysts behaved similarly except for SOL derived sample that in the fresh form, where the protective agent is still present, showed a higher selectivity toward glyceric acid at the expense of tartronic acid. PVA in fact is known to be able to direct the adsorption-desorption of glycerol favouring the mono-oxidation. To be noted that Table 4 reported only the most relevant products. All the other minor products showed selectivity less than 10%.

3. Conclusion

With the aim to study the ruling factor for developing synergism between Au and Ag in the selective glycerol oxidation, we prepared 1%AuAg/TiO₂ at internal Au:Ag 1:1 and 4:1 ratio by two different techniques namely DPU and SOL immobilisation. Both techniques present some peculiarities:

DPU use a sequential deposition where Ag is deposited on the support first and then Au is added whereas SOL immobilisation technique forms the metallic particles in solution (avoiding AgCl precipitation) and then supporting them. The results highlighted different starting materials, the one (DPU) with markedly higher Au/Ag atomic ratio at the surface than the other (SOL). We studied the evolution of the systems by thermal treatment in different atmosphere (H_2 and air). In the case of SOL samples we observed sintering during calcination with an increase of particle size from 2.7/2.9 nm to 5.3/5.1 nm depending on the Au/Ag ratio. The particle size of thermally treated DPU samples were 2.6/2.4 nm. UV-vis, XPS and CO-DRIFT have been carried out highlighting quite surprising similarities between calcined and reduced samples. In particular, it seems that thermal treatment induced the establishing of SMSI which become the ruling factor determining the oxidation state of the metal. The 1%Au₄Ag₁/TiO₂_DPU both reduced and calcined presented almost the same distribution of metals with the same oxidation state.

Correlating the catalytic behaviour and the characterization performed to the catalysts we could conclude that the ratio between Au and Ag on the surface of the particles is fundamental for developing a synergistic effect. In fact, all the catalysts tested with an internal ratio of 1:1 resulted inactive. In particular, the composition of the catalyst should be always gold-rich. The presence of larger amount of Au compared to Ag, allows the Ag to be more stable in the reduced form even in an oxidative environment. The particle size does not appear very important at least in the range here investigated (2–5 nm) while more relevant appeared the exposure of the metals, being the gold preferred. Moreover, the synergy between Au and Ag can be also mediated by the presence of Au^{δ+} which can be always formed through the interaction with the support.

Acknowledgements

We want to thank Viridiana Maturano for DPU samples preparation. RZ thanks DGAPA-UNAM IN103719 project for financial support.

Conflict of Interest

The authors declare no conflict of interest.

Keywords: AuAg bimetallic catalyst · synergistic effect · glycerol oxidation

- [1] Z. Bhusan N. H. David, D. N. Matthew, D. Robert, *Science* **2010**, *330*, 74–78.
- [2] P. Gallezot, *Catal. Today* **1997**, *37*, 405–418.
- [3] A. Behr, J. Eilting, K. Irawadi, J. Leschinski, F. Lindner, *Green Chem.* **2008**, *10*, 13–30.
- [4] C. H. Zhou, J. N. Beltramini, Y. X. Fan, G. Q. Lu, *Chem. Soc. Rev.* **2008**, *37*, 527–549.
- [5] S. Carrettin, P. McMorn, P. Johnston, K. Griffin, C. J. Kiely, G. J. Hutchings, *Phys. Chem. Chem. Phys.* **2003**, *5*, 1329–1336.
- [6] F. Porta, L. Prati, *J. Catal.* **2004**, *224*, 397–403.
- [7] S. E. Davis, M. S. Ide, R. J. Davis, *Green Chem.* **2013**, *15*, 17–45.
- [8] P. Konova, A. Naydenov, C. Venkov, D. Mehandjiev, D. Andreeva, T. Tabakova, *J. Mol. Catal. A Chem.* **2004**, *213*, 235–240.
- [9] F. Yang, M. S. Chen, D. W. Goodman, *J. Phys. Chem. C* **2009**, *113*, 254–260.
- [10] D. E. Starr, S. K. Shaikhutdinov, H.-J. Freund, *Top. Catal.* **2005**, *36*, 33–41.
- [11] A. J. Wang, X. F. Zhang, L. Y. Jiang, L. Zhang, J. J. Feng, *ChemCatChem* **2018**, *10*, 3319–3326.
- [12] X.-Y. Huang, A.-J. Wang, X.-F. Zhang, L. Zhang, J.-J. Feng, *ACS Appl. Energy Mater.* **2018**, *1*, 5779–5786.
- [13] Y. C. Shi, J. J. Feng, X. X. Lin, L. Zhang, J. Yuan, Q. L. Zhang, A. J. Wang, *Electrochim. Acta* **2019**, *293*, 504–513.
- [14] H. You, Z. Wu, Y. Jia, X. Xu, Y. Xia, Z. Han, Y. Wang, *Chemosphere* **2017**, *183*, 528–535.
- [15] C. Louis, *Catalysts* **2016**, *6*, 110.
- [16] J.-H. Liu, A.-Q. Wang, Y.-S. Chi, H.-P. Lin, C.-Y. Mou, *J. Phys. Chem. B* **2005**, *109*, 40–43.
- [17] A. Sandoval, A. Aguilar, C. Louis, A. Traverse, R. Zanella, *J. Catal.* **2011**, *281*, 40–49.
- [18] T. Yonezawa, N. Toshima, *New J. Chem.* **1998**, *22*, 1179–1201.
- [19] L. Deng, W. Hu, H. Deng, S. Xiao, J. Tang, *J. Phys. Chem. C* **2011**, *115*, 11355–11363.
- [20] T. J. A. Slater, A. Macedo, S. L. M. Schroeder, M. G. Burke, P. O'Brien, P. H. C. Camargo, S. J. Haigh, *Nano Lett.* **2014**, *14*, 1921–1926.
- [21] C. Méthivier, R. Zanella, C. Louis, L. Delannoy, A. Sandoval, *Appl. Catal. A* **2015**, *504*, 287–294.
- [22] F. Somodi, L. Prati, A. Balerna, C. Evangelisti, A. Beck, A. Villa, G. Nagy, C. Tiozzo, A. Jouve, *J. Catal.* **2018**, *368*, 324–335.
- [23] T. Benkó, A. Beck, K. Frey, D. F. Srankó, O. Geszti, G. Sáfrán, B. Maróti, Z. Schay, *Appl. Catal. A* **2014**, *479*, 103–111.
- [24] R. Zanella, L. Delannoy, C. Louis, *Mechanism of Deposition of Gold Precursors onto TiO₂ during the Preparation by Cation Adsorption and Deposition-precipitation with NaOH and Urea*, **2005**.
- [25] R. Zanella, C. Louis, *Catal. Today* **2005**, *107–108*, 768–777.
- [26] F. Bonaccorso, M. Zerbetto, A. C. Ferrari, V. Amendola, *J. Phys. Chem. C* **2013**, *117*, 13217–13229.
- [27] A. M. Ferraria, A. P. Carapeto, A. M. Botelho do Rego, *Vacuum* **2012**, *86*, 1988–1991.
- [28] K. H. Hr. Klimev, K. Fajerweg, K. Chakarova, L. Delannoy, C. Louis, *J. Mater. Sci.* **2007**, *42*, 3299–3306.
- [29] S. Campisi, C. E. Chan-Thaw, D. Wang, A. Villa, L. Prati, *Catal. Today* **2016**, *278*, 91–96.

Manuscript received: April 1, 2019

Revised manuscript received: May 14, 2019

Accepted manuscript online: May 16, 2019

Version of record online: June 12, 2019